SCIENTIFIC ARTICLE

Quantitative MRI in patients with gluteal tendinopathy and asymptomatic volunteers: Initial results on T1- and T2*-mapping diagnostic accuracy and correlation with clinical assessment.

Joseph Rudy Dadour [1], Guillaume Gilbert [1, 2], Marianne Lepage-Saucier [3], Véronique Freire [1], Nathalie J Bureau [1, 4]

Corresponding author : Nathalie J Bureau (nathalie.bureau@umontreal.ca)

[1] Department of Radiology, Centre hospitalier de l'Université de Montréal (CHUM), 1000 rue Saint- Denis, Montreal, Quebec H2X 0C1, Canada

[2] MR Clinical Science, Philips Canada, Markham, Ontario L6C 2S3, Canada

[3] Department of Radiology, Hôpital Pierre-Boucher, 1333 Boulevard Jacques-Cartier Est, Longueuil, Quebec J4M 2A5, Canada

[4] Research Center, Centre hospitalier de l'Université de Montréal (CHUM), 900 rue Saint-Denis, Montreal, Quebec H2X 0A9, Canada

ABSTRACT

Objective. To determine if T1- and T2*-mapping of the gluteal tendons can discriminate between participants with and without clinical findings of gluteal tendinopathy (GT) and if they correlate with clinical assessment.

Materials and Methods. This prospective study was conducted between January and December 2016. MRI of the hip included Spin Echo, Short-T1 Inversion Recovery, variable-flip angle and variable echo-time gradient echo sequences. MRI studies were reviewed independently by two radiologists. Two other readers segmented the gluteal tendons and T1, mono- ($T2^*_m$) and bi-exponential T2* [short ($T2^*_s$) and long ($T2^*_l$) components] were computed.

Results. Ten participants with GT [median age; interquartile range: 63 (57 – 67) years, all women] and 9 participants without GT [57 (55 – 59) years, 8 women] ($P = 0.06$) were enrolled. The sensitivity and specificity of reader 1 for disease classification were 40% [95% confidence interval (CI): 17% – 61%], 70% (CI: 47% – 91%) and that of reader 2 were 70% (CI: 43% – 86%), 80% (CI: 53% – 96%), with fair inter-reader agreement (Kappa = .38). T1 values could not discriminate between the two groups. The gluteal tendons $T2^*_m$ and $T2^*_s$ showed diagnostic accuracy ranging from .80 to .89. The posterior gluteus medius tendon $T2^*_m$ and $T2^*_s$ respectively showed sensitivity and specificity of 90%, and strong correlation (Spearman's *rho* = -.71; $P = 0.02$) with the *Lower Extremity Functional Scale* score.

Conclusion. Quantitative MRI could help gain new insight into healthy and diseased gluteal tendons to allow better diagnosis and treatment stratification for patients.

Keywords: Magnetic resonance imaging; T1-mapping, T2*-mapping; Tendinopathy; Tendinosis; Gluteal tendons.

INTRODUCTION

Gluteal tendinopathy (GT) affects between 10 and 25% of people over 50 years of age, with a fivefold increased risk in women. [1] GT refers to lateral hip pain with tenderness on palpation of the greater trochanter area and difficulty walking and climbing stairs. [2] This disorder is the result of degenerative changes and overload of the gluteus medius (Gmed) and/or gluteus minimus (Gmin) tendons leading to tendinosis and in some cases, to partial or full-thickness tears. [3]

Imaging can help diagnose patients with GT. The accuracy of both ultrasound and magnetic resonance imaging (MRI) in identifying advanced structural lesions of gluteal tendinosis such as full-thickness tears, is good, but their ability to detect early changes and partial tears remains limited. [4] Moreover, these techniques can be criticized for their reliance on a qualitative and subjective assessment of images and their poor correlation with the presence of pain and the severity of symptoms. [5, 6]

Because normal tendons are composed of highly organized collagen fibers, which have a low free proton content and a majority of short T2/T2* components, they appear low-signal or dark with clinical imaging techniques. [7] In other words, the signal from tendon tissue decays very rapidly while the relatively long echo times (TE), greater than 10 milliseconds (ms) used in conventional MRI, limit the opportunity to detect short T2/T2* signals before they become null. [8] Consequently, the capability of conventional MRI to depict the internal structure of tendons is restricted. To overcome this limitation, Ultrashort Echo Time (UTE) [9] imaging sequences allowing image acquisition at TEs less than 1 ms have been developed, and standard cartesian gradient echo (GE) sequences [10, 11] have been optimized to achieve short TEs less than 10 ms. These sequences can be used to objectively characterize tendons by measuring various MRI

parameters, including longitudinal T1 and transverse T2* relaxation times. UTE and short-TE GE sequences used to quantitatively evaluate healthy and diseased Achilles tendons have shown promising results when assessing the early stages of tendinosis [12-14] and could potentially help to assess GT. Therefore, the aim of this study was to investigate T1- and T2*-mapping in gluteal tendons in vivo. We hypothesized that T1 and T2* values of the lateral and posterior Gmed tendons, and of the Gmin tendon, estimated from variable-flip angle and variable echo-time GE sequences respectively, could discriminate between participants with and without clinical symptoms and signs of GT. Furthermore, we hypothesized that quantitative MRI parameters in participants with GT would correlate with clinical assessment.

MATERIALS AND METHODS

This prospective study was approved by the Centre hospitalier de l'IUniversité de Montréal review board (CE 15.244) and all participants signed written informed consent.

Participants

Three physiatrists, each with more than 30 years of experience and working in outpatient clinics, recruited participants with a clinical diagnosis of GT. Potentially eligible individuals were invited to participate in the study if they met all of the following criteria: 1) aged $\geq$ 18 years old; 2) presence of lateral hip pain for at least 3 months; 3) tenderness on palpation of the greater trochanter area; 4) pain during resisted isometric hip abduction and/or pain with passive hip adduction; 5) average pain score over the past seven days upon walking and climbing stairs of $\geq$ 4 on a 0 (no pain) to 10 (worst pain imaginable) numerical rating scale.

Potentially eligible participants were excluded if they had a history of: 1) trauma to the affected hip in the last 4 weeks; 2) hip or lumbar spine surgery; 3) pelvis or affected hip fracture;

4) moderate to severe osteoarthritis or avascular necrosis of the affected hip; 5) rheumatoid or seronegative arthritis; 6) fibromyalgia; 7) corticosteroid injection to the affected hip within the past 3 months; 8) local infection in the affected hip joint area; 9) contraindication to MRI. In eligible participants with bilateral GT, the most symptomatic hip was imaged for the study. An age-matched group of participants reporting no history of any symptoms in both hips and who did not meet the exclusion criteria were recruited from the hospital community by the investigators.

Clinical assessment

The participants completed the *Lower Extremity Functional Scale* (LEFS) questionnaire. [15]

MRI scanning protocol

All MRI acquisitions were performed on a clinical 3T system (Achieva X-series, Philips Healthcare, Best, The Netherlands), using the integrated body-coil for excitation and a 16-channel surface coil for signal reception. Patients were placed supine with their hands resting on their chest. Mild internal rotation of the hips (approximately 15 degrees) was achieved by taping the patients' toes. Quantitative T2* mapping was undertaken using a multi-echo, variable echo-time, slab-selective 3D GE sequence [14]. Two multi-echo sequences with 6 TEs each were acquired, for a total of 12 TEs = 1.1, 2.8, 4.5, 6.2, 7.9, 9.6, 11.3, 13.0, 14.7, 16.4, 18.1 and 19.8 ms. Other acquisition parameters were: TR= 46 ms, FOV= 154 mm x 154 mm x 72 mm , spatial resolution= 0.6 mm x 0.8 mm x 3 mm, flip angle= 18°, bandwidth= 785.7 Hz/pixel , acquisition time= 11min 24sec. Quantitative T1-mapping was performed using a variable-flip angle GE sequence with coverage and spatial resolution identical to the T2*-mapping sequence. Other parameters were: TR= 29 ms, TE=1.15 ms, flip angles = 5, 15 and 25°, acquisition time = 9 min 39sec. A B1+ map was acquired using the actual-flip angle method to allow transmit field

inhomogeneity correction during post-processing. Given that the hip is a large anatomical region, slab-selective excitation was chosen to limit signal generation to the area of the gluteal tendons thus precluding the need for extensive signal oversampling that would have prolonged the acquisition time significantly. The conventional MRI sequences are listed in **Table 1**.

Conventional MRI analysis

The MRI studies were de-identified and stored in the Picture Archiving and Communication System (PACS). Two fellowship-trained musculoskeletal radiologists with 5 and 8 years of experience respectively, blinded to the clinical status of the participants, independently reviewed the MRI studies using a grading system. **(Table 2)** This system is based on previously described MRI features of GT [5] and grading of muscular fatty infiltration. [16] The radiologists were asked to assess the greater trochanteric bursa, the gluteal tendons and the gluteal muscles individually, and to classify each study participant as having or not GT based on their overall assessment.

Quantitative MRI data analysis

A fellowship-trained musculoskeletal radiologist with 23 years of experience and a second year radiology resident, blinded to the clinical status of the participants, independently segmented the entire volume of the Gmed and Gmin tendons on the 3D GE T2* maps using the ITK-SNAP 3.2 image segmentation tool. [17] A rigid registration performed between the sequences used for T2*- and T1- mapping prior to data analysis automatically transferred the segmentations between the two series.

An MRI physicist with 10 years of experience, blinded to the clinical status of the participants, performed the post-processing computer analysis of the short-TE GE images. The quantitative T2* values were estimated on a voxel-by-voxel basis using nonlinear regression to

both a mono-exponential model ($T2^*_m$) and a bi-exponential model (short $T2^*_s$ and long $T2^*_l$). The quantitative T1 values were estimated on a voxel-by-voxel basis using the methodology developed by Grosse et al. [12] and incorporating a correction for transmit field inhomogeneities using information from the acquired B1+ map. Calculations of the T2* and T1 maps were implemented in Matlab R2016b (The Mathworks, Natick, MA, USA).

Statistical analysis

Descriptive statistics were calculated for the participants' demographic characteristics and LEFS scores. Median and interquartile range (IQR) were computed for the MRI parameters of each individual tendon and for all three tendons combined. Fisher's exact test or the Mann-Whitney *U*-test were used to test for significant differences between the participants with and without GT. The sensitivity and specificity of MRI findings with their 95% confidence interval (CI) were calculated using clinical diagnosis as the reference standard. Inter-reader agreement was assessed using Cohen's Kappa (κ). Receiver operating characteristic (ROC) curve analysis was used to assess the diagnostic accuracy of the MRI parameters at discriminating participants with and without GT. The Dice coefficient (DC) was used to evaluate the reproducibility of the manual contouring of the gluteal tendons by the two readers. [18] Interpretation of the DC and κ was based on Landis and Koch. [19] The linear relationship between the MRI parameters and the LEFS scores was evaluated using Spearman's rho correlation coefficient (*rho*). The analyses were performed with SPSS software (IBM SPSS Statistics, version 24; IBM Corp, Armonk, NY) using a two-tailed test and a significance level of 5%.

RESULTS

Participants

Between January and December 2016, 12 participants with and 9 participants without GT were enrolled in the study. Two participants with GT were excluded: one for severe hip osteoarthritis, and the other for claustrophobia. The final groups included 10 women with GT (median age; IQR: 63; 57 – 67 years) and 8 women and one man without GT (median age; IQR: 57; 55– 59 years). One participant without GT had both hips imaged. Median age (P = 0.06) and sex distribution (P >.99) were comparable between groups. **(Table 3)**

Conventional MRI studies

The results of the sensitivity, specificity and inter-reader agreement for the interpretation of the MRI findings by the two radiologists are included in **Table 4**. In terms of diagnostic accuracy, reader 1 had a sensitivity of 40% (CI: 17% – 61%) and a specificity of 70% (CI: 47% – 91%) when discriminating between participants with and without GT, whereas reader 2 had a sensitivity of 70% (CI: 43% – 86%) and a specificity of 80% (CI: 53% – 96%). For both readers, the greater trochanteric bursa was the most sensitive [reader 1 and 2: 100% (CI: 76% – 100%)], although poorly specific [reader 1 and 2: 50% (CI: 26% – 50%)] MRI finding. **(Fig. 1)** Inter-reader reliability values were lowest for the Gmed posterior tendon assessment (κ = -.02; CI: -.19 – .16) with poor agreement, and were highest for the greater trochanteric bursa (κ = 1.00; CI: .42 – 1.00) with perfect inter-reader agreement. **(Fig. 2)** Gmin and Gmed muscle fatty infiltration, as indirect signs of GT, showed high specificity for both readers, ranging from 80% to 100%, with substantial (κ = .77) and moderate (κ = .55) inter-reader agreement, respectively.

Quantitative MRI data

Table 5 presents the results of quantitative MRI parameters for the gluteal tendons and **Fig. 3** shows representative quantitative maps in participants with and without GT. For each investigated tendon and all three tendons combined the median T1 value was lower in

participants with GT compared with participants without GT. However, the difference between both groups only reached statistical significance for the lateral Gmed tendon median T1 value. For the T1 parameter, area under the ROC values ranged from .21 (CI: .00 – .44) for the lateral Gmed tendon to .43 (CI: .17 – .69) for the posterior Gmed tendon.

The T2* values were computed using the models with mono- and bi-exponential fits (**Fig. 4)**. For each investigated tendon and all three tendons combined, the median $T2^*_m$ and median $T2^*_s$ values were significantly higher in participants with GT compared with participants without GT. The $T2^*_l$ parameter did not reach statistical significance. For the $T2^*_m$ parameter, the area under the ROC values ranged from .81 (CI: .62 – 1.00) for the Gmin tendon to .89 (CI: .72 – 1.00) for the posterior Gmed tendon. For the $T2^*_s$ parameter, the area under the ROC values ranged from .80 (CI: .60 – .99) for the posterior Gmed tendon to .89 (CI .75 – 1.00) in all three tendons combined. **(Fig. 5)** The mean DC of all the segmentation pairs was .69 (range: .56 – .80) for the posterior Gmed tendon corresponding to substantial agreement, and .55 (range: .24 – .73) for the lateral Gmed tendon and .59 (range: .38 – .72) for the Gmin tendon, both corresponding to moderate agreement. There was no statistically significant difference between the mean DC of the paired segmentations in participants with GT compared with participants without GT.

Correlation between quantitative MRI parameters and LEFS score

In participants with GT, there was a strong negative correlation (*rho* = -.71; CI: -.93 – -.14; *P* = 0.02) between the posterior Gmed tendon $T2^*_s$ parameter and the LEFS score, with higher $T2^*_s$ values associated with lower values of LEFS score and therefore with higher level of functional disability. LEFS score did not correlate with any other quantitative MRI parameter nor in any other tendons.

DISCUSSION

Gluteal tendinopathy (GT) is the primary cause of lateral hip pain and may lead to physical impairment similar to people with end-stage hip osteoarthritis. [2] Therapeutic management of GT is still debated, paralleling the lack of relevant markers to assist the clinicians treating these patients. [20] MRI is the best modality to investigate GT but it has played a minor role in the early detection of the disease and treatment monitoring so far. [21] In this study, 2 musculoskeletal radiologists reviewing MRI studies of participants with and without GT obtained low to moderate sensitivity (40% and 70%) and moderate specificity (70% and 80%) with fair inter-reader agreement ($\kappa = .38$) at discriminating between the two groups. Furthermore, inter-reader agreement was poor (-.02) for the assessment of the posterior gluteus medius (Gmed) tendon, fair (0.38) for the lateral Gmed tendon and substantial (0.68) for the gluteus minimus (Gmin) tendon. Because of the small sample size resulting in wide 95% confidence intervals, we must remain cautious in the interpretation of these results. Nevertheless, these results suggest that conventional MRI in patients with signs and symptoms of GT has limited diagnostic accuracy and relies on subjective analysis of structural findings. Moreover, other authors have reported the limited performance of MRI at differentiating between tendinosis, partial and complete tears of the Gmed tendon, with sensitivity of 65% and specificity of 67% when compared to surgery and histopathology. [4]

Quantitative MRI studies have shown promising results for the characterization of Achilles [14, 22] and of rotator cuff [23, 24] tendinopathy. Furthermore, MRI parameters have been shown to correlate with clinical scores in Achilles tendinopathy [14] and with the mechanical properties of tendons [25]. In this study, variable flip-angle and variable echo-time GE sequences were used to investigate T1- and T2*-mapping, respectively. We found

statistically significant lower T1 values in the lateral gluteus medius (Gmed) tendon of participants with GT compared with asymptomatic controls. However, the performance of T1 values at discriminating between the two groups was poor. Other studies investigating the Achilles tendon in patients with chronic tendinopathy [13] and with spondyloarthropathy [26] using UTE techniques have shown good diagnostic accuracy of T1 values. However, in the present study, the long acquisition time for UTE sequences, precluded the use of this technique in our protocol. Instead we used short TE sequences where the T1 relaxation time is influenced by the T2* component of the imaged tissue, which could explain the lower sensitivity in detecting changes associated with tendon pathology. [26] In that respect, our results concur with those of Bachmann et al. who also showed that T1-mapping with short TE sequences could not detect subtle changes in tendinosis induced by cross-linking in a phantom model. [25]

We performed the mono- and bi-exponential calculation of T2* and demonstrated that the mono $T2^*_m$ and short $T2^*_s$ components were better at distinguishing between participants with and without GT, than the long $T2^*_l$ component. Tendons are highly organized collagenous tissues comprising distinct water compartments with different relaxation times. [27] The $T2^*_s$ component relates to water bound macromolecules and the $T2^*_l$ component to free water. [28] As tendon degeneration progresses, the proportion of bound water relative to free water increases, elevating the $T2^*_s$ component. [29-32] As the mono-exponential calculation of T2* provides a weighted mean value of both compartments' relaxation times, it may underestimate the changes that occur in tendon degeneration, especially in the early stage of the disease. In this study however, $T2^*_m$ proved to have discriminative properties. This might be the result of having a majority of long-standing cases that could present more evidence of advanced tendon pathology. Both $T2^*_m$ and $T2^*_s$ components performed well at discriminating between

participants with and without clinical findings of GT with diagnostic accuracy ranging from .80 to .89. Considering that the biochemical changes that accompany aging were likely to be present in the tendons of our control group of asymptomatic middle- to advanced-age people these markers appear to have the ability to discriminate between symptomatic pathological changes and asymptomatic age-related physiological changes in the gluteal tendons.

In this study, the posterior Gmed tendon $T2^*_m$ parameter showed very good diagnostic performance with sensitivity and specificity of 90% at a threshold of 13.11 ms, whereas the $T2^*_s$ parameter was strongly correlated with clinical assessment (*rho* = -.71; *P* = 0.02). These findings support the clinical relevance of quantitative MRI for the characterization of GT.

The inter-reader agreement for the manual segmentation of the gluteal tendons was greatest for the posterior Gmed tendon, both in participants with and without GT. The inter-reader agreement was substantial [.69 (range: .56 – .80)] in keeping with the fact that this tendon is the largest and most easily recognizable of the gluteal tendons. Conversely, the smaller structures of the lateral Gmed component and of the Gmin tendon were more difficult to segment because of limited image resolution. This may have caused volume averaging with surrounding muscle and other tissues to interfere with the method's accuracy in those tendons.

There are some limitations to this study. Firstly, the generalizability of our findings is limited by the small sample size. Studies with larger sample size allowing patient stratification according to the various stages of GT and to the specific gluteal tendon involved, are needed to validate these research findings. Secondly, there was no surgical nor histopathological reference standard. Gluteal tendinopathy was diagnosed based on clinical symptoms and signs, which is the currently recognized clinical approach. Thirdly, manual segmentation of the gluteal tendons is time consuming and represents a limitation to the clinical translation of quantitative MRI

markers. In this study, manual segmentation of all three gluteal tendons was an hour long task. However, our results suggest that segmentation could be limited to the posterior Gmed tendon, which is the largest of the gluteal tendons and the easiest to segment. This could significantly reduce the time for manual segmentation and could facilitate the introduction of deep learning-based segmentation algorithms. Lastly, studies have shown that T2* of tendons are influenced by the magic angle effect and by magnetic field inhomogeneities. [33, 34] However, with the patient in the supine position for MRI, the gluteal tendons are naturally aligned in a direction parallel to B0 and the magic angle may not be as much of an issue for these tendons as it is for the rotator cuff.

In conclusion, mono and short T2* relaxation time measurements of the gluteal tendons showed good to very good diagnostic performance at discriminating between participants with and without gluteal tendinopathy. The sensitivity and specificity of the mono T2* component of the posterior gluteus medius tendon was 90%, respectively. The short T2* component of the posterior gluteus medius tendon correlated strongly with clinical assessment. Quantitative MRI could help gain new insight into healthy and diseased gluteal tendons to allow better diagnosis and treatment stratification for patients. Further studies with larger sample size are required to validate these results.

ACKNOWLEDGEMENTS

The authors wish to thank gratefully Ms. Kathleen Beaumont for providing manuscript editorial assistance and Mr. Marc Dorais for providing statistical analysis assistance.

FUNDING

Nathalie J Bureau (#266408) is supported by a Clinical Research Scholarship from the Fonds de recherche du Québec – Santé (FRQ-S) and the Fondation de l'association des radiologistes du Québec (ARQ).

CONFLICT OF INTEREST

The authors declare no competing interests.

REFERENCES:

1. Segal NA, Felson DT, Torner JC, Zhu Y, Curtis JR, Niu J, et al. Greater trochanteric pain syndrome: epidemiology and associated factors. Archives of physical medicine and rehabilitation. 2007; 88(8):988-992.

2. Fearon AM, Cook JL, Scarvell JM, Neeman T, Cormick W, Smith PN. Greater trochanteric pain syndrome negatively affects work, physical activity and quality of life: a case control study. The Journal of arthroplasty. 2014; 29(2):383-386.

3. Kingzett-Taylor A, Tirman PF, Feller J, McGann W, Prieto V, Wischer T, et al. Tendinosis and tears of gluteus medius and minimus muscles as a cause of hip pain: MR imaging findings. AJR American journal of roentgenology. 1999; 173(4):1123-1126.

4. Docking SI, Cook J, Chen S, Scarvell J, Cormick W, Smith P, et al. Identification and differentiation of gluteus medius tendon pathology using ultrasound and magnetic resonance imaging. Musculoskelet Sci Pract. 2019; 41:1-5.

5. Blankenbaker DG, Ullrick SR, Davis KW, De Smet AA, Haaland B, Fine JP. Correlation of MRI findings with clinical findings of trochanteric pain syndrome. Skeletal radiology. 2008; 37(10):903-909.

6. Woodley SJ, Nicholson HD, Livingstone V, Doyle TC, Meikle GR, Macintosh JE, et al. Lateral hip pain: findings from magnetic resonance imaging and clinical examination. The Journal of orthopaedic and sports physical therapy. 2008; 38(6):313-328.

7. Bydder GM. Review. The Agfa Mayneord lecture: MRI of short and ultrashort T(2) and T(2)* components of tissues, fluids and materials using clinical systems. Br J Radiol. 2011; 84(1008):1067-1082.

8. Chang EY, Du J, Chung CB. UTE imaging in the musculoskeletal system. Journal of magnetic resonance imaging : JMRI. 2015; 41(4):870-883.

9. Robson MD, Gatehouse PD, Bydder M, Bydder GM. Magnetic resonance: an introduction to ultrashort TE (UTE) imaging. Journal of computer assisted tomography. 2003; 27(6):825-846.

10. Deligianni X, Bar P, Scheffler K, Trattnig S, Bieri O. High-resolution Fourier-encoded sub-millisecond echo time musculoskeletal imaging at 3 Tesla and 7 Tesla. Magnetic resonance in medicine : official journal of the Society of Magnetic Resonance in Medicine / Society of Magnetic Resonance in Medicine. 2013; 70(5):1434-1439.

11. Deligianni X, Bar P, Scheffler K, Trattnig S, Bieri O. Water-selective excitation of short T2 species with binomial pulses. Magnetic resonance in medicine : official journal of the Society of Magnetic Resonance in Medicine / Society of Magnetic Resonance in Medicine. 2014; 72(3):800-805.

12. Grosse U, Springer F, Hein T, Grozinger G, Schabel C, Martirosian P, et al. Influence of physical activity on T1 and T2* relaxation times of healthy Achilles tendons at 3T. Journal of magnetic resonance imaging : JMRI. 2015; 41(1):193-201.

13. Grosse U, Syha R, Hein T, Gatidis S, Grozinger G, Schabel C, et al. Diagnostic value of T1 and T2 * relaxation times and off-resonance saturation effects in the evaluation of Achilles tendinopathy by MRI at 3T. Journal of magnetic resonance imaging : JMRI. 2015; 41(4):964-973.

14. Juras V, Apprich S, Szomolanyi P, Bieri O, Deligianni X, Trattnig S. Bi-exponential T2 analysis of healthy and diseased Achilles tendons: an in vivo preliminary magnetic resonance study and correlation with clinical score. European radiology. 2013; 23(10):2814-2822.

15. Binkley JM, Stratford PW, Lott SA, Riddle DL. The Lower Extremity Functional Scale (LEFS): scale development, measurement properties, and clinical application. North American Orthopaedic Rehabilitation Research Network. Physical therapy. 1999; 79(4):371-383.

16. Goutallier D, Postel JM, Bernageau J, Lavau L, Voisin MC. Fatty muscle degeneration in cuff ruptures. Pre- and postoperative evaluation by CT scan. Clinical orthopaedics and related research. 1994(304):78-83.

17. Yushkevich PA, Piven J, Hazlett HC, Smith RG, Ho S, Gee JC, et al. User-guided 3D active contour segmentation of anatomical structures: significantly improved efficiency and reliability. Neuroimage. 2006; 31(3):1116-1128.

18. Zou KH, Warfield SK, Bharatha A, Tempany CM, Kaus MR, Haker SJ, et al. Statistical validation of image segmentation quality based on a spatial overlap index. Acad Radiol. 2004; 11(2):178-189.

19. Landis JR, Koch GG. The measurement of observer agreement for categorical data. Biometrics. 1977; 33(1):159-174.

20. Del Buono A, Papalia R, Khanduja V, Denaro V, Maffulli N. Management of the greater trochanteric pain syndrome: a systematic review. Br Med Bull. 2012; 102:115-131.

21. Grimaldi A, Mellor R, Hodges P, Bennell K, Wajswelner H, Vicenzino B. Gluteal Tendinopathy: A Review of Mechanisms, Assessment and Management. Sports Med. 2015; 45(8):1107-1119.

22. Grosse U, Syha R, Martirosian P, Wuerslin C, Horger M, Grozinger G, et al. Ultrashort echo time MR imaging with off-resonance saturation for characterization of pathologically altered Achilles tendons at 3 T. Magnetic resonance in medicine : official journal of the Society

of Magnetic Resonance in Medicine / Society of Magnetic Resonance in Medicine. 2013; 70(1):184-192.

23. Ashir A, Ma Y, Jerban S, Jang H, Wei Z, Le N, et al. Rotator Cuff Tendon Assessment in Symptomatic and Control Groups Using Quantitative MRI. Journal of magnetic resonance imaging : JMRI. 2020.

24. Ganal E, Ho CP, Wilson KJ, Surowiec RK, Smith WS, Dornan GJ, et al. Quantitative MRI characterization of arthroscopically verified supraspinatus pathology: comparison of tendon tears, tendinosis and asymptomatic supraspinatus tendons with T2 mapping. Knee Surg Sports Traumatol Arthrosc. 2016; 24(7):2216-2224.

25. Bachmann E, Rosskopf AB, Gotschi T, Klarhofer M, Deligianni X, Hilbe M, et al. T1- and T2*-Mapping for Assessment of Tendon Tissue Biophysical Properties: A Phantom MRI Study. Invest Radiol. 2019; 54(4):212-220.

26. Wright P, Jellus V, McGonagle D, Robson M, Ridgeway J, Hodgson R. Comparison of two ultrashort echo time sequences for the quantification of T1 within phantom and human Achilles tendon at 3 T. Magnetic resonance in medicine : official journal of the Society of Magnetic Resonance in Medicine / Society of Magnetic Resonance in Medicine. 2012; 68(4):1279-1284.

27. Cameron IL, Short NJ, Fullerton GD. Verification of simple hydration/dehydration methods to characterize multiple water compartments on tendon type 1 collagen. Cell Biol Int. 2007; 31(6):531-539.

28. Du J, Diaz E, Carl M, Bae W, Chung CB, Bydder GM. Ultrashort echo time imaging with bicomponent analysis. Magnetic resonance in medicine : official journal of the Society of

Magnetic Resonance in Medicine / Society of Magnetic Resonance in Medicine. 2012; 67(3):645-649.

29. Docking S, Samiric T, Scase E, Purdam C, Cook J. Relationship between compressive loading and ECM changes in tendons. Muscles, ligaments and tendons journal. 2013; 3(1):7-11.

30. Jarvinen M, Jozsa L, Kannus P, Jarvinen TL, Kvist M, Leadbetter W. Histopathological findings in chronic tendon disorders. Scandinavian journal of medicine & science in sports. 1997; 7(2):86-95.

31. Riley G. The pathogenesis of tendinopathy. A molecular perspective. Rheumatology. 2004; 43(2):131-142.

32. Scott JE. Extracellular matrix, supramolecular organisation and shape. J Anat. 1995; 187 (Pt 2):259-269.

33. Du J, Chiang AJ, Chung CB, Statum S, Znamirowski R, Takahashi A, et al. Orientational analysis of the Achilles tendon and enthesis using an ultrashort echo time spectroscopic imaging sequence. Magn Reson Imaging. 2010; 28(2):178-184.

34. Du J, Pak BC, Znamirowski R, Statum S, Takahashi A, Chung CB, et al. Magic angle effect in magnetic resonance imaging of the Achilles tendon and enthesis. Magn Reson Imaging. 2009; 27(4):557-564.

Table 1: Conventional MRI scanning protocol.

Parameters	STIR pelvis	SE T1 pelvis	SE FS T2 hip
Orientation	Axial	Coronal	Coronal
TE (ms)	80	10	70
TR (ms)	25530	535	2313
IR (ms)	210		
Flip angle (degrees)	90	90	90
FOV (mm)	380	400	160
Slice thickness (mm)	6	4	3.5
Matrix	336 x 327	508 x 504	204 x 202
Acquisition time (min:sec)	06:48	06:11	04:37
Averages	1	2	3
Bandwidth (Hz/pixel)	592	690	692.3

SE = spin echo; STIR = short-T1 inversion recovery; FS = fat saturated; TE = echo time; TR = repetition time; IR = inversion recovery time; FOV = field of view.

Table 2: Conventional MRI findings grading system.

Imaging features	Grading score	
Greater trochanteric bursa	• Grade 0:	Normal
	• Grade 1:	T2 hyperintensity
	• Grade 2:	Bursitis (fluid distension of the greater trochanteric bursa)
Gmin tendon	• Grade 0:	Normal
	• Grade 1:	Tendinosis (abnormal increased signal intensity within the tendon on T1w images with or without thickening of the tendon)
	• Grade 2:	Partial tear (T2 hyperintensity within the tendon with or without thinning of the tendon)
	• Grade 3:	Complete tear (discontinuity of the tendon with or without osseous avulsion)
Gmed lateral tendon	• Grade 0:	Normal
	• Grade 1:	Tendinosis (abnormal increased signal intensity within the tendon on T1w images with or without thickening of the tendon)
	• Grade 2:	Partial tear (T2 hyperintensity within the tendon with or without thinning of the tendon)
	• Grade 3:	Complete tear (discontinuity of the tendon with or without osseous avulsion)
Gmed posterior tendon	• Grade 0:	Normal
	• Grade 1:	Tendinosis (abnormal increased signal intensity within the tendon on T1w images with or without thickening of the tendon)
	• Grade 2:	Partial tear (T2 hyperintensity within the tendon with or without thinning of the tendon)
	• Grade 3:	Complete tear (discontinuity of the tendon with or without osseous avulsion)
Gmin muscle on coronal T1w	• Grade 0:	Normal, without fatty streaks
	• Grade 1:	Some fatty streaks
	• Grade 2:	Fatty infiltration (more muscle than fat)
	• Grade 3:	Fatty infiltration (equal amount of fat and muscle)
	• Grade 4:	Fatty infiltration (more fat than muscle)
Gmed muscle on coronal T1w	• Grade 0:	Normal, without fatty streaks
	• Grade 1:	Some fatty streaks
	• Grade 2:	Fatty infiltration (more muscle than fat)
	• Grade 3:	Fatty infiltration (equal amount of fat and muscle)
	• Grade 4:	Fatty infiltration (more fat than muscle)
Diagnostic impression	•	Participant without GT
	•	Participant with GT

Gmin : gluteus minimus; Gmed : gluteus medius; T1w : spin echo T1-weighted sequence; GT : gluteal tendinopathy.

Table 3: Characteristics of participants with and without gluteal tendinopathy.

	Groups		*P**
Variables	**With gluteal tendinopathy**	**Without gluteal tendinopathy**	
Participants, N	10	9	
Sex, N (%)			
Men	0 (0)	1 (11)	>.99
Women	10 (100)	8 (89)	
Hips, N (%)	10 (100)	10 (100)	
Age (years), median (IQR)	63 (57 – 67)	57 (55 – 59)	0.06
BMI (kg/m^2), median (IQR)	25.6 (24.1 – 28.6)	21.7 (21.5 – 22.9)	0.01
Side, N (%)			
Right	6 (60)	7 (70)	>.99
Left	4 (40)	3 (30)	
Symptoms' duration (months), median (IQR)	12 (12 – 18)	0	
LEFS, median (IQR)	41 (21 – 50)	80 (80 – 80)	<0.001

N = number; IQR = Interquartile range; BMI = body mass index. *Fisher's exact test or Mann-Whitney *U*-test. The *Lower Extremity Functional Scale* (LEFS) score is calculated out of 80, with a lower score indicating a worse status.

Table 4: Sensitivity, specificity and inter-reader agreement for conventional MRI findings.

	Reader 1		Reader 2		κ
Imaging findings	**Sensitivity(%) (95% CI)**	**Specificity(%) (95% CI)**	**Sensitivity(%) (95% CI)**	**Specificity(%) (95% CI)**	**Dichotomous grading score[a] (95% CI)**
Greater trochanteric bursa	100 (76 – 100)	50 (26 – 50)	100 (76 – 100)	50 (26 – 50)	1.00 (.42 – 1.00)
Gmin tendon	50 (25 – 66)	80 (55 – 96)	70 (44 – 80)	90 (64 – 100)	.68 (.14 – .88)
Gmed lateral tendon	60 (34 – 83)	40 (17 – 64)	90 (64 – 100)	70 (44 – 80)	.38 (-.15 – .77)
Gmed posterior tendon	20 (4 – 20)	100 (84 – 100)	70 (44 – 90)	60 (34 – 80)	-.02 (-0.19 – 0.16)
Gmin muscle fatty infiltration	50 (25 – 66)	80 (55 – 96)	50 (26 – 50)	100 (76 – 100)	.77 (.21 – .77)
Gmed muscle fatty infiltration	40 (18 – 40)	100 (78 – 100)	80 (55 – 80)	100 (75 – 100)	.55 (.04 – .55)
Diagnostic impression	40 (17 – 61)	70 (47 – 91)	70 (43 – 86)	80 (53 – 96)	.38 (-.14 – .71)

κ = Cohen's kappa; 95% CI = 95% confidence interval; Gmin = Gluteus minimus; Gmed = Gluteus medius. [a]Imaging findings with multiple categories were assessed as dichotomized data in 0 versus ≥ 1, or in 0, 1 versus ≥ 2 in the case of Gmin and Gmed muscle fatty infiltration.

Table 5. Results of quantitative MRI parameters analysis of the gluteal tendons.

		Groups		*P**
	Tendon	**With gluteal tendinopathy (N = 10)**	**Without gluteal tendinopathy (N = 10)**	
T1, ms	Gmin	1403.25 (1250.31 – 1635.50)	1469.33 (1334.89 – 1600.14)	0.545
	Gmed lateral	1414.83 (1240.79 – 1553.50)	1669.30 (1602.21 – 1769.16)	0.028
	Gmed posterior	1285.35 (1224.58 – 1509.89)	1411.00 (1260.04 – 1497.58)	0.597
	Combined	1378.89 (1308.24 – 1514.52)	1549.13 (1424.13 – 1616.42)	0.082
Mono-exponential T2*, ms	Gmin	16.07 (13.55 – 19.89)	13.27 (12.22 – 15.07)	0.019
	Gmed lateral	19.17 (18.12 – 22.93)	16.62 (14.82 – 18.07)	0.007
	Gmed posterior	14.00 (13.26 – 15.30)	12.77 (12.21 – 12.99)	0.003
	Combined	16.73 (15.17 – 18.74)	14.07 (13.18 – 15.19)	0.004
Bi-exponential short T2*, ms	Gmin	10.33 (8.16 – 13.79)	7.12 (6.96 – 7.96)	0.007
	Gmed lateral	11.22 (10.42 – 13.48)	8.40 (7.57 – 10.64)	0.005
	Gmed posterior	7.62 (6.36 – 9.02)	6.46 (5.81 – 7.24)	0.023
	Combined	10.08 (8.34 – 11.52)	7.33 (6.67 – 8.54)	0.003
Bi-exponential long T2*, ms	Gmin	23.81 (18.89 – 25.34)	21.24 (20.12 – 24.68)	0.762
	Gmed lateral	26.33 (24.16 – 29.64)	26.69 (21.76 – 28.49)	0.450
	Gmed posterior	23.01 (21.07 – 24.99)	22.37 (21.15 – 23.92)	0.762
	Combined	23.90 (23.04 – 26.52)	23.42 (21.61 – 24.95)	0.326

ms = milliseconds; combined data of both readers are presented as median (interquartile range);
*Mann-Whitney *U* test.

FIGURES

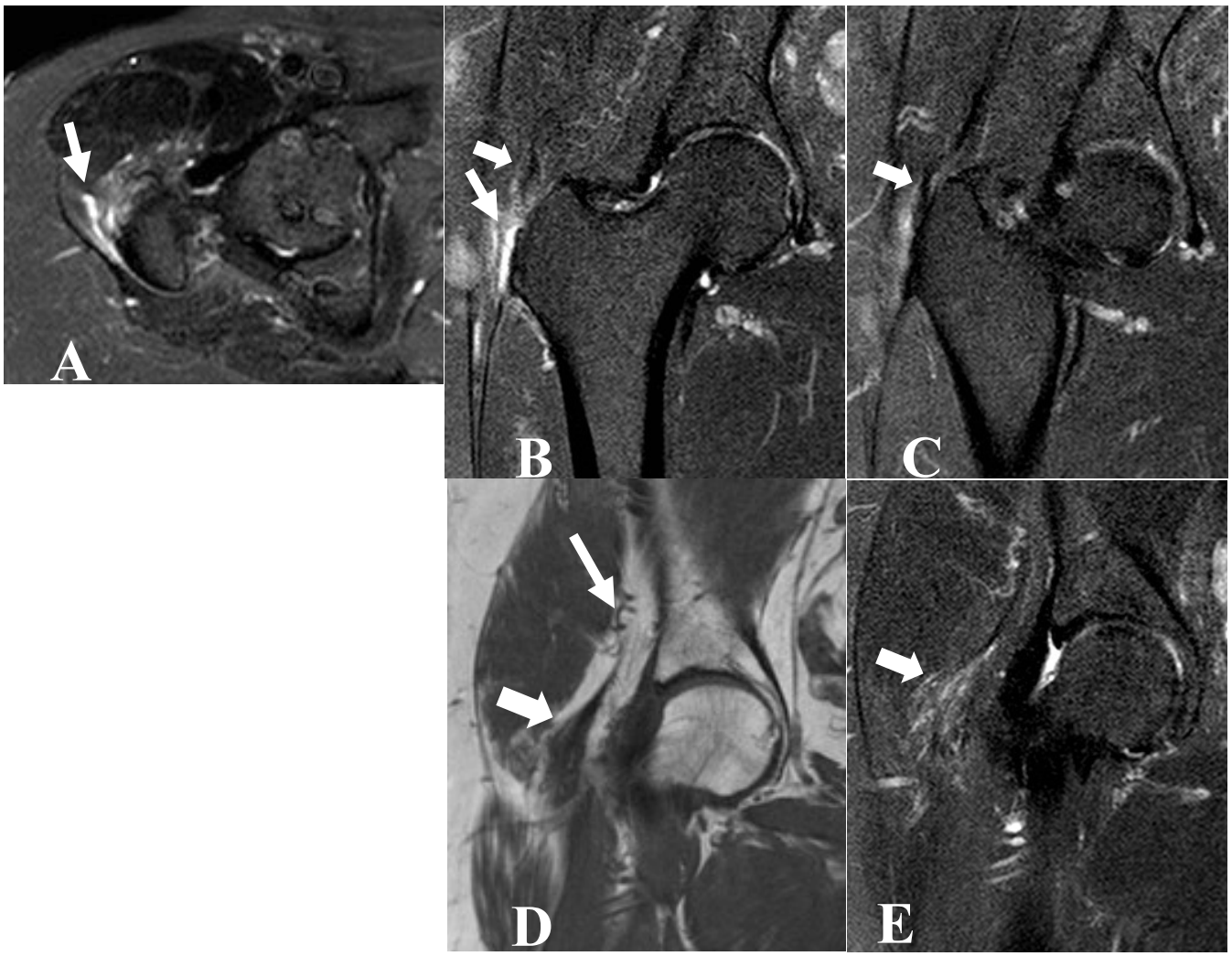

Fig. 1a Conventional MRI in a 67-year-old woman with right hip chronic gluteal tendinopathy identified by both readers as a patient. Axial STIR image shows fluid distension of the greater trochanteric bursa (arrow). Both readers identified this finding as a grade 2 lesion (bursitis). **b** Coronal fat-suppressed T2-weighted image demonstrates hyperintense signal at the lateral facet of the greater trochanter (thin arrow) and an irregular, partially-retracted lateral gluteus medius tendon (thick arrow). **c** A more posterior image shows the tendon attaching to the facet (thick arrow). One reader diagnosed a lateral gluteus medius grade 1 lesion (tendinosis) whereas the other reader diagnosed a grade 3 (complete tear) lesion. **d** Coronal T1-weighted image depicts fatty infiltration of the gluteus minimus muscle (thin arrow) identified as a grade 4 lesion (more fat than muscle) by both readers. The gluteus minimus tendon (thick arrow) shows increased signal intensity and thickening. **e** Corresponding coronal fat-suppressed T2-weighted image demonstrates increased signal in the area of the gluteus minimus tendon (thick arrow). One reader diagnosed a gluteus minimus grade 1 lesion (tendinosis) whereas the other reader reported a grade 2 lesion (partial tear).

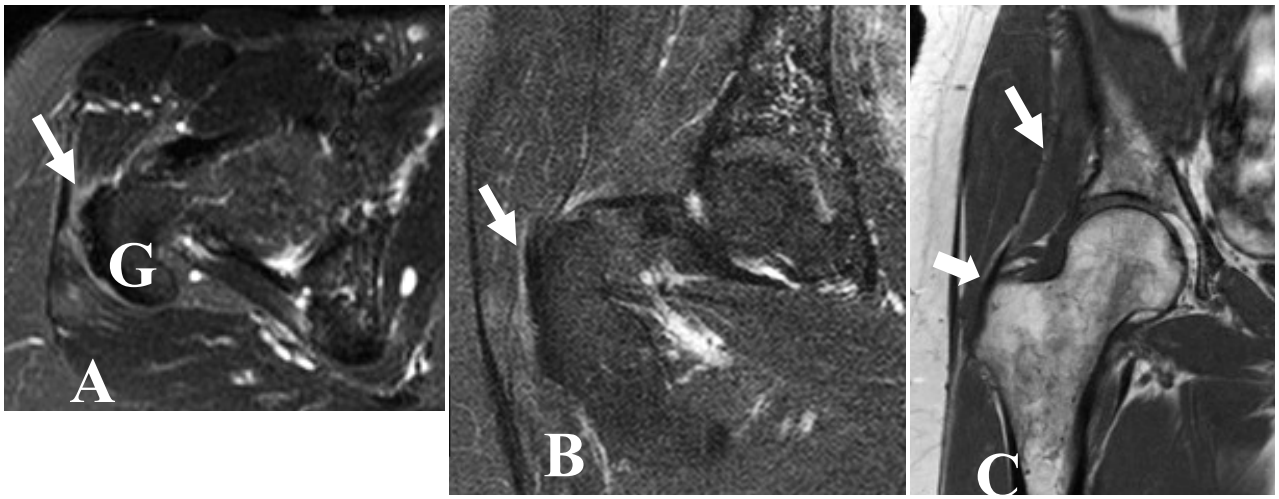

Fig. 2a Conventional MRI in a 64-year-old asymptomatic woman's right hip, identified by both readers as an asymptomatic volunteer. Axial STIR image shows hyperintensity (arrow) adjacent to the greater trochanter (G). Both readers identified this finding as a grade 1 lesion (T2 hyperintensity) of the greater trochanteric bursa. **b** Coronal fat-suppressed T2-weighted image demonstrates the lateral gluteus medius tendon attaching to the lateral facet of the greater trochanter (thin arrow). One reader diagnosed a lateral gluteus medius grade 1 lesion (tendinosis) whereas the other reader indicated a normal tendon (grade 0). **c** Coronal T1-weighted image depicts the gluteus minimus muscle (thin arrow) and tendon (thick arrow). Both readers graded the gluteus minimus muscle and tendon as normal (grade 0).

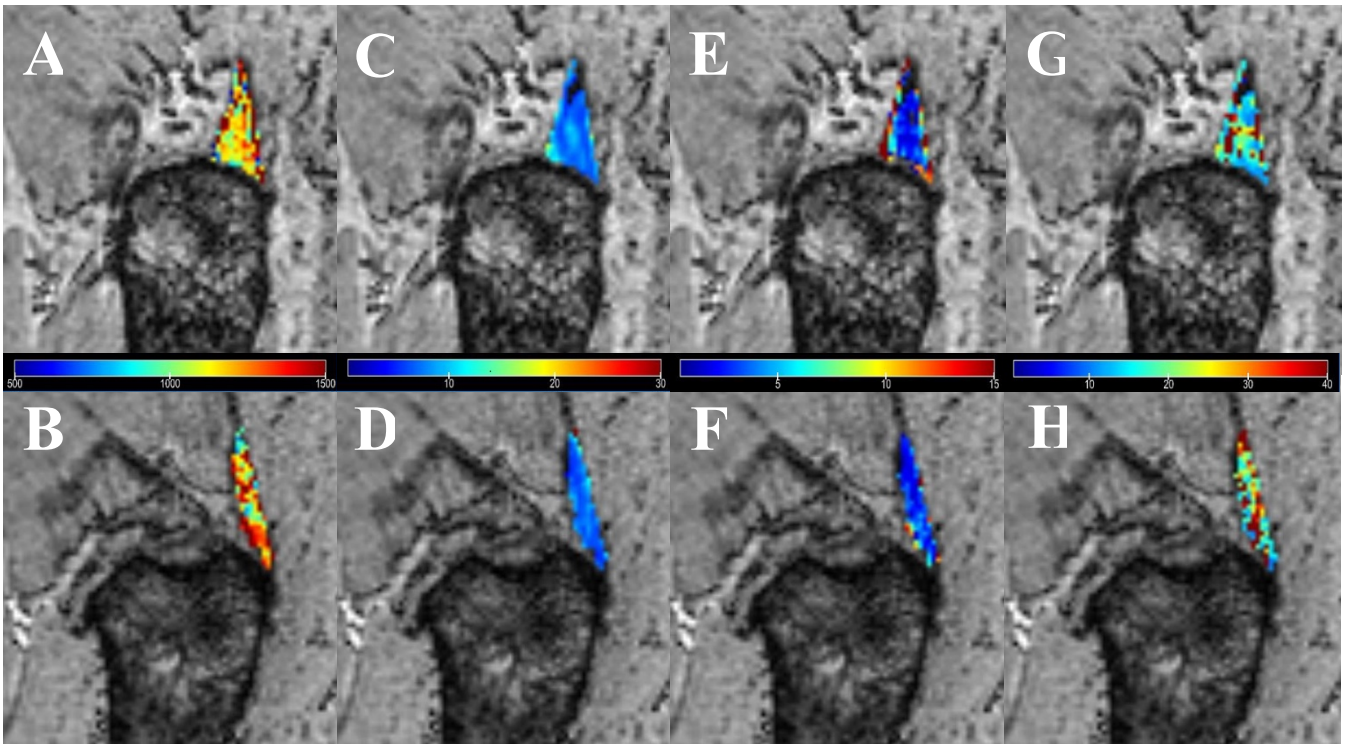

Fig. 3 Representative 2D quantitative maps in a 70-year-old woman with right hip chronic gluteal tendinopathy (upper row) and in a 64-year-old asymptomatic woman's right hip (same subject as figure 2) (bottom row). **a** and **b** correspond to calculated T1; **c** and **d** correspond to mono-exponentially calculated T2*; **e** and **f** correspond to the short component of T2*; **g** and **h** correspond to the long component of T2*. Individual quantitative maps are overlaid on sagittal short-TE gradient echo images. In some cases, the visual difference between the patient's and volunteer's maps may appear subtle. This may be explained by the small overall absolute differences between both groups and because a single image of a 3D set of images of each map is presented herein. Furthermore, the comparison is limited to two subjects. The maps' units are in milliseconds. TE = echo time.

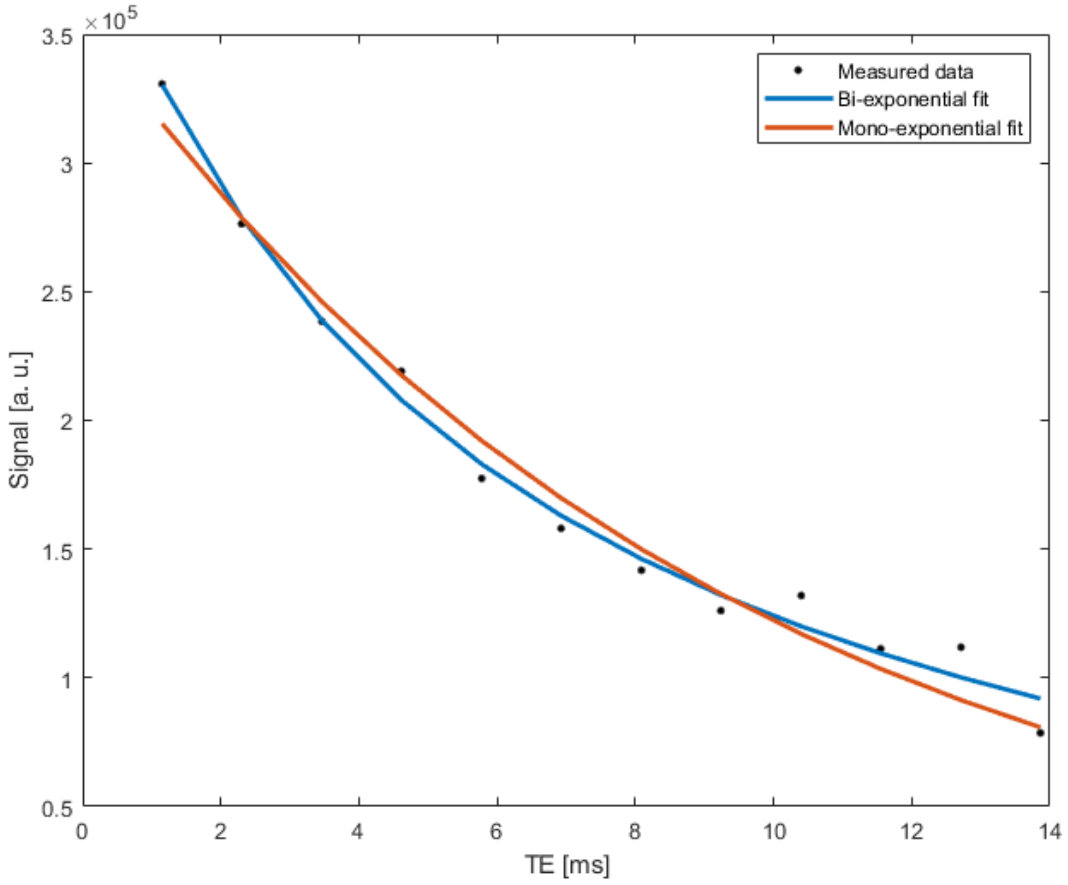

Fig. 4. Example of the fit quality for one voxel in the gluteus medius tendon of a 61-year-old woman with right hip chronic gluteal tendinopathy. The blue line represents the bi-exponential fit of the data and the red line represents the mono-exponential fit of the data. R^2 was 0.9889 for the bi-exponential fit and 0.9772 for the mono-exponential fit.

R^2 = R-squared (coefficient of determination); Signal [a.u.] = signal [arbitrary units]; TE [ms] = echo time [milliseconds].

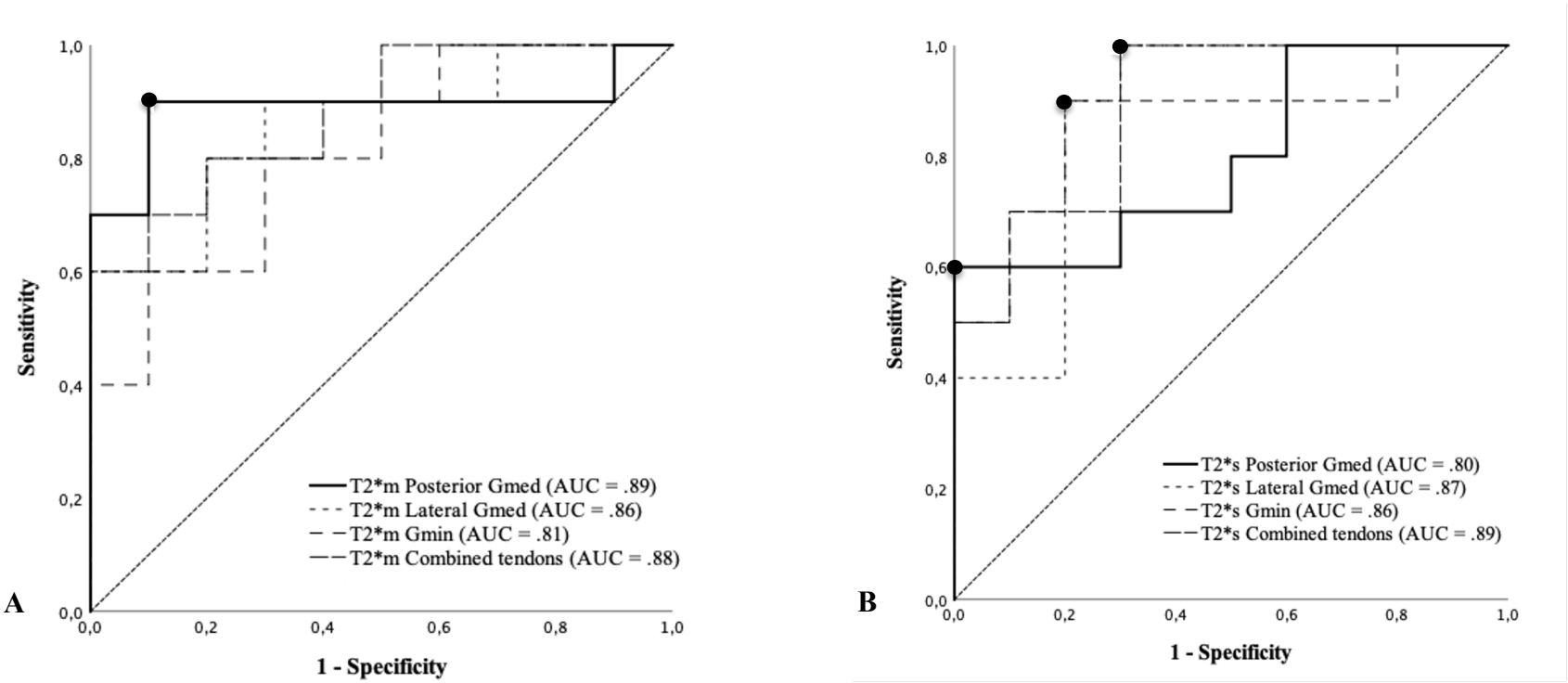

Fig. 5a. ROC curves and diagnostic accuracy (AUC) for $T2^*_m$ of each tendon and all three tendons combined in 10 participants with and 9 participants without gluteal tendinopathy. As determined by the optimal operating points, $T2^*_m$ of the posterior Gmed tendon showed the best diagnostic performance at a threshold of 13.11 ms, with sensitivity and specificity of 90% respectively. **Fig. 5b.** Corresponding ROC curves and diagnostic accuracy (AUC) for the $T2^*_s$ parameter. The diagnostic performance of the $T2^*_s$ of the lateral Gmed and Gmin tendons was similar with sensitivity of 90% and specificity of 80%, at a threshold of 10.39 ms and 7.84 ms respectively. Comparatively, $T2^*_s$ of all three tendons combined had higher sensitivity 100% but lower specificity 70% at a threshold of 7.87 ms, whereas $T2^*_s$ of the posterior Gmed tendon had lower sensitivity 60% but higher specificity 100% at a threshold of 7.53 ms. Gmed = gluteus medius; Gmin = gluteus minimus; AUC = area under the ROC.